Proceedings of the ASME 2010 3rd Joint US-European Fluids Engineering Summer Meeting and 8th International Conference on Nanochannels, Microchannels, and Minichannels
FEDSM-ICNMM2010
August 1-5, 2010, Montreal, Canada

FEDSM-ICNMM2010-31210

LONG TERM DYNAMICS OF WATER-ENTRY CAVITY

Roderick R. La Foy
Dept. of Mechanical Engineering,
Virginia Polytechnic Institute and State University,
Blacksburg, VA, USA

Sunghwan Jung
Dept. of Engineering Science and Mechanics,
Virginia Polytechnic Institute and State University,
Blacksburg, VA, USA

Pavlos Vlachos
Dept. of Mechanical Engineering,
Virginia Polytechnic Institute and State University,
Blacksburg, VA, USA

ABSTRACT

Many engineering applications involve the motion of objects crossing a fluid interface. The dynamics of this process are often complicated due to the interplay of surface tension, gravity, and inertia. Nevertheless, a simple analysis using potential flow theory works well to predict the interfacial profile of the air cavity formed during an impact. Most current theories however, cannot predict the behavior of the air cavity after pinch off occurs. We therefore investigated the long term dynamics of water entry in both experiment and theory. It was found that shortly after pinch off the cavity dynamics become governed primarily by thermodynamic gas relations. The internal pressure slowly rises due to the cavity volume decreasing while the ambient liquid pressure quickly increases as a result of the descent of the projectile. This effect is incorporated into our model to correctly predict the cavity geometry.

INTRODUCTION

The impact and penetration of objects through water-air free surfaces has been observed in many engineering applications, and the dynamics of this process have challenged scientists and engineers for over a century. Early work by Worthington [1, 2] and von Karman [3] laid the foundation for many subsequent investigations on the impact of a body with a liquid free surface that spanned a wide range of phenomena and processes. Some engineering applications of interest include ship slamming [4], ocean structure-wave interaction [5], and ballistics [6, 7]. Other examples including the locomotion of the basilisk lizard across the free surface [8] and skipping stones on water [9, 10] illustrate the far reaching relevance of water entry problems. Many engineering designs also involve fluid-structure interactions at the free surface [3, 6, 11, 12]. In military applications, designs are created that minimize impact forces generated on missiles or planes impinging on free surfaces [13]. Several additional problems include the interface dynamics of bodies exiting the free surface [5, 17, 18], forced wetting-dewetting [14, 15], and surface coating processes [16].

The dynamics of water-entry processes are influenced by multiple forces including the hydrostatic pressure, the surface tension, and the surface chemistry of the projectile. In this work, the short-term cavity model is expanded to include both radial and axial surface tension terms. Additionally the long term dynamics are also captured by including the interfacial pressure discontinuity that appears after pinch-off.

Many previous studies have ignored the effects of surface tension and surface chemistry, but when the cavity radius decreases as occurs during pinch-off or if the projectile diameter approaches the capillary length, the surface tension forces are no longer negligible. The surface tension forces are related to the two principle curvatures of the liquid-gas interface. Most current models use only the in-plane (horizontal) curvature and neglect the out-of-plane (vertical) curvature. Taking into account the out-of-plane curvature results in a non-trivial partial differential equation that can be transformed into an ordinary differential equation by assuming that the projectile velocity remains constant.

Additionally earlier work including the hydrostatic pressure forces only capture the short-term cavity dynamics

[19-21]. During the descent of the projectile the cavity closes separating part of the cavity from the free surface atmosphere. Once this occurs, the cavity profile becomes governed by the pressure difference across the fluid interface. This pressure difference is primarily determined by the depth of the closure event. In this work the potential flow model is improved by incorporating this pressure difference while both the short and long term dynamics of the analytical model are compared to experimental data.

THEORETICAL MODEL

Our theoretical model expands on previous work by including several additional forces acting on the cavity. In contrast to previous studies investigating water impact events, we focus on the dynamics of the air cavity after the closure event (which is also referred to as pinch-off or deep seal) while simultaneously including both the radial and axial surface tension terms.

Initial theory describing the cavity radius in cavitation and bubble dynamics was derived by Lord Rayleigh [23] in 1917. Duclaux *et. al.* [19] in 2007 expanded these models to include the transient dynamics of the cavity assuming a potential flow solution. The profile of this model agreed well with experiments for projectiles with various shapes and wetting properties. Unfortunately, this model is not applicable to the dynamics after pinch-off due to the influence of pressure upon the closed volume of air. As the cavity is compressed, the pressure increases following the polytropic gas law (Abelson [24]). Additionally previous work has not accounted for the effect of surface tension on the cavity shape. The recent paper by Aristoff *et. al.* [20] considers the effect of in-plane surface tension while neglecting the out-of-plane component. The proposed mathematical model in this study advances upon previous work [19-21] to more accurately describe the cavity profile.

In this work we will first incorporate the effect of surface tension into the potential flow solutions. Preliminary results including the surface tension show that this effect is not negligible even with large Weber numbers (on the order of 50 or higher). We will then extend the cavity model beyond pinch-off by including the effect of the internal cavity pressure in the solution.

Surface Tension Effects

Using a potential flow model, the profile of an axisymmetric air cavity may be described by the following equation [19, 20]

$$R\ddot{R}+\frac{3}{2}\dot{R}^2=\frac{p_f(z)-p_\infty(z)}{\rho} \qquad (1)$$

where R is the radius of air cavity, ρ is the fluid density, p_∞ is the fluid pressure at a large horizontal distance from the air cavity, and p_f is the fluid pressure at the air-liquid interface. In general the far field pressure p_∞ may be a function of time, but during a water impact, the pressure in the liquid is given by $p_\infty(z)=p_{atm}+\rho g z$ and is therefore independent of time.

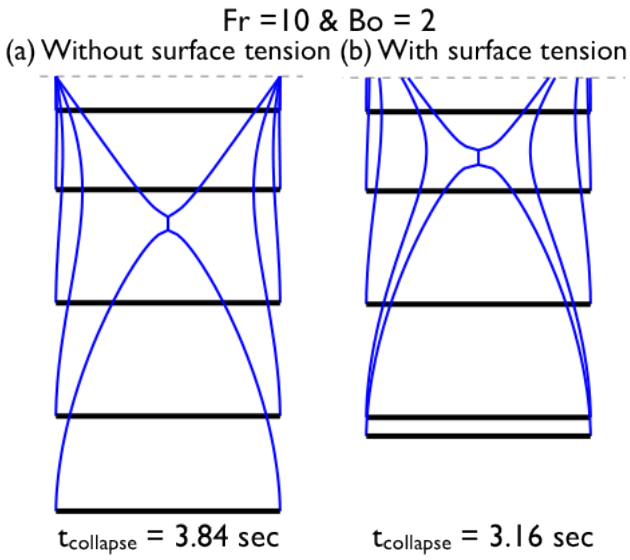

FIGURE 1: Graphs comparing the analytical model with and without surface tension included. (a). Without surface tension the pinch-off occurs later and at a greater depth than (b). with the surface tension included.

With the surface tension terms included in the model, the pressure becomes

$$p_f(z)=p_a(z)-\sigma\left(\frac{1}{R}-\frac{\partial^2 R}{\partial z^2}\right) \qquad (2)$$

where p_a is the internal air pressure and σ is the interfacial surface tension. Before pinch-off, when the cavity is open to the atmosphere, $p_a(R)$ is assumed to be approximately equal to p_{atm}. Substituting the modified pressure containing the surface tension terms into equation (1) yields a partial differential equation. This PDE may be simplified by noting that if the velocity of the projectile is assumed to be constant, then the second order spatial derivative of R is proportional to the second order time derivative of R or $U\partial_z \sim \partial_t$. Using this relationship, the governing differential equation may be written in non-dimensional form as

$$\left(R-\frac{1}{We_D}\right)\ddot{R}+\frac{3}{2}\dot{R}^2=-\frac{1}{Fr_z}-\frac{1}{R}\frac{1}{We_D} \qquad (3)$$

where R is the radius of cavity non-dimensionalized by the diameter of the projectile D, and Fr_z and We_D are the Froude and Weber numbers defined by

$$Fr_z=\frac{U^2}{g z}$$

$$We_D=\frac{\rho U^2 D}{\sigma} \qquad (4)$$

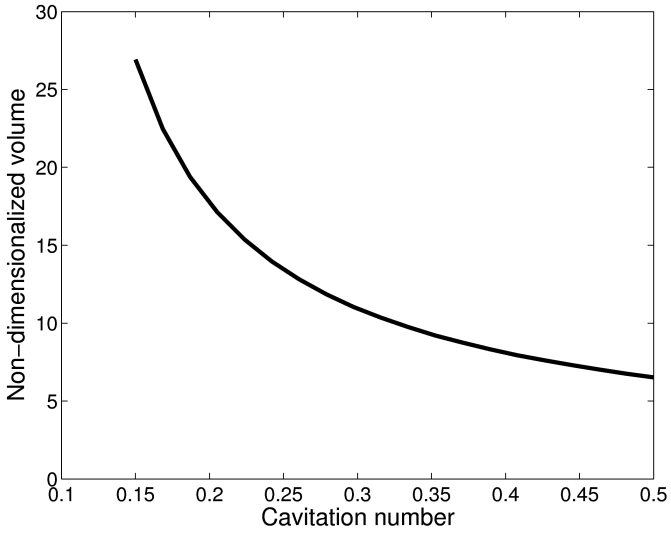

FIGURE 2: The non-dimensional volume of the cavity after pinch-off as a function of the cavity pressure coefficient.

thus the solution of this differential equation is a function of the depth z. This equation can be solved using boundary conditions

$$R(0)=1$$
$$\frac{dR(0)}{dt}=\alpha=\frac{1}{\tan(\theta_c-\pi/2)} \qquad (5)$$

where θ_c is the contact angle of the fluid on the surface of the projectile.

Once a cavity is formed, the surface chemistry of the projectile becomes dominant in determining the cavity profile. The advancing contact angle provides a boundary condition on the cavity which causes large volumes of entrained air for hydrophobic surfaces. Larger contact angles tend to cause the pinch-off depth to increase. The contact angle may also depend on the projectile velocity as a relationship between these variables was shown in experimental measurements of the flow around a cavitation bubble [25, 26]. However the contact angle in falling projectiles has not been well characterized experimentally.

In the limit of the surface tension going to zero (or the limit of the Weber number going to infinity), equation (3) simplifies to the model derived by Duclaux et. al. [19]. For We < 100, the effect of surface tension is non-negligible and the predicted cavity profile becomes wider with pinch-off occurring later than when surface tension is included as illustrated in Fig. 1.

Dynamics of the Sealed Cavity

Eventually as the projectile descends through the liquid, the cavity closes. The portion of the cavity that remains attached to the projectile will no longer be sustained at atmospheric pressure. The work by Duclaux et. al. [19] assumed the internal cavity pressure remained constant and was equal to the hydrostatic pressure. In this model it is assumed that the air pressure is lower than the ambient liquid pressure since the hydrostatic pressure will be higher than the atmospheric pressure. The non-dimensionalized governing equation including the pressure discontinuity on the interface is given by

$$\left(R-\frac{1}{We_D}\right)\ddot{R}+\frac{3}{2}\dot{R}^2=-2c-\frac{1}{Fr_z}-\frac{1}{R}\frac{1}{We_D} \qquad (6)$$

where c is a cavity pressure coefficient defined by the function

$$c=\frac{p_\infty(z_{pinch-off})-p_a}{\rho U^2/2} \qquad (7)$$

and $z_{pinch-off}$ is the depth of the closure event below the free surface.

The pressure inside the cavity p_a is assumed to be constant while the exterior liquid pressure p_∞ linearly depends upon the depth of cavity closure. Thus the parameter c is a function of the pinch-off depth and the projectile's velocity. As the pressure coefficient increases, the volume of the cavity after pinch-off decreases as shown in Fig. 2. Therefore, the volume of the cavity is directly related to the depth of the pinch-off event. Fig. 3 shows shadowgraph images of the cavity profile shortly after pinch-off. In these images, the volume of the cavity dramatically increases with larger velocities. The solution of equation (6) may be found using the boundary conditions given by expression (5).

EXPERIMENTS

A series of flow visualization experiments were conducted to investigate the unsteady flow dynamics during water entry and to compare with the theoretical model. In these tests a series of spheres passed through the free surface while a high-speed camera recorded shadowgraph images of the body and surrounding fluid. To investigate the effects of

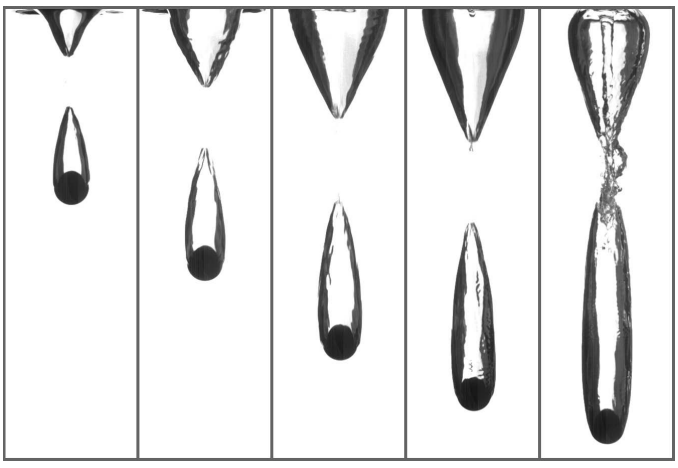

FIGURE 3: The cavity profiles shown 1 ms after pinch-off for different impact speeds. In the sequence, the velocity increases from left to right.

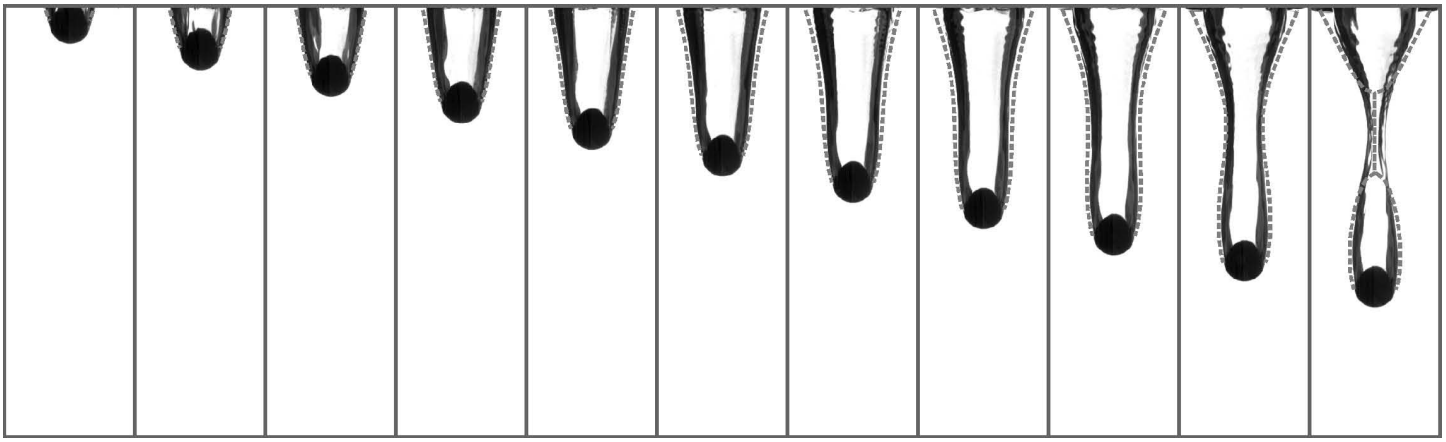

FIGURE 4: A time sequence showing a 1.11 cm (7/16 in) diameter hydrophobic sphere impacting a free surface at 1.79 m/s with the analytical model plotted over the shadowgraph images. The images are spaced 4 ms apart in time and span from 2 ms to 46 ms after impact.

wetting angle on the flow structure, bodies with both hydrophilic and hydrophobic surfaces were tested. The setup used a 37 L glass tank lit from behind with a diffused 1000 W spotlight. The spheres were released from multiple heights to control the impact velocity. To minimize the angular velocity of the projectiles during impact, the spheres were released from a slowly opened camera iris. This resulted in highly repeatable tests. The spheres that were tested in this study were chrome plated steel ball bearings.

Before tests, the spheres were cleaned with acetone, isopropyl alcohol, and ethanol to remove any oils that could result in inhomogeneous wetting angles. For the hydrophobic tests, the spheres were coated with WX2100 (manufactured by Cytonix Co.). This coating creates a surface with a static wetting angle of 122 degrees. The impact velocities were varied from approximately 1 m/s to 3.5 m/s. The high-speed video was taken with a Photron APX RS camera at 5000 fps at a resolution of 1024 by 512 pixels.

During the tests conducted with the hydrophilic spheres, no cavities were formed for the velocity range tested. This result is in agreement with earlier work that found that cavities will not form with hydrophilic projectiles below approximately 8 m/s [19].

In contrast to the hydrophilic cases, the hydrophobic projectile impacts result in highly dynamic cavities. As the sphere descends, the water-air contact line rotates towards the back of the sphere. Eventually the hydrostatic pressure along with the surface tension cause the cavity to collapse [22], resulting in pinch-off. Both shallow and deep seal behaviors [20] were apparent for the parameter range studied. For the cases with low Bond numbers, Bo=0.14, longitudinal waves in the cavity were apparent as described by Aristoff, *et al* [20].

To compare the experimental data to the theoretical model, several experimental parameters were extracted from the high-speed video. The most important of these parameters was the exact impact velocity. The general velocity range was controlled by varying the drop height of the projectiles, but the exact velocities varied by up to 1.8% of the mean velocity. The velocity measurements were taken by fitting a circular arc to the spheres in the images. The edge of the sphere was found using the Canny edge detection algorithm while the fitting procedure was completed using a least-squares regression. From the fitting parameters determined for each frame, the velocity of the sphere could be determined to subpixel accuracy.

In addition to measuring the impact velocity from the high-speed video, the pinch-off depth, the pinch-off time, and the cavity volume were also determined using similar image processing techniques.

RESULTS

The primary objective of this work was to expand the theoretical cavity model to include both the full surface tension forces and the dynamics of the cavity after pinch-off. In order to validate these changes to the model, the solutions to equation (6) are compared to experimental data taken from the shadowgraph tests.

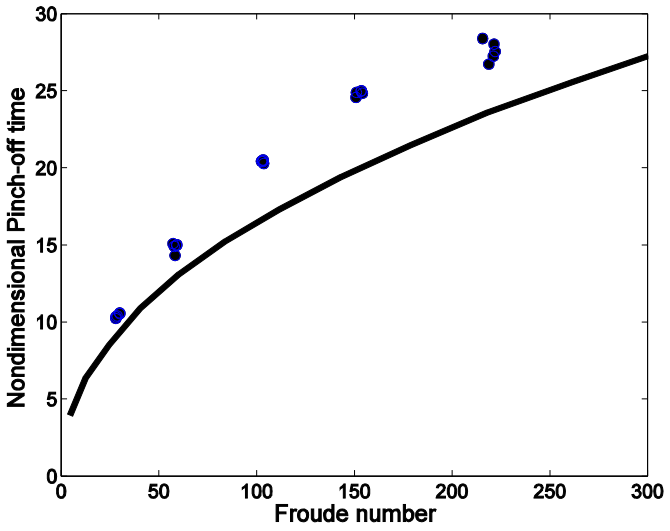

FIGURE 5: The non-dimensional pinch-off time as a function of the Froude number. The line corresponds to the analytical model and the dots to the experimental data.

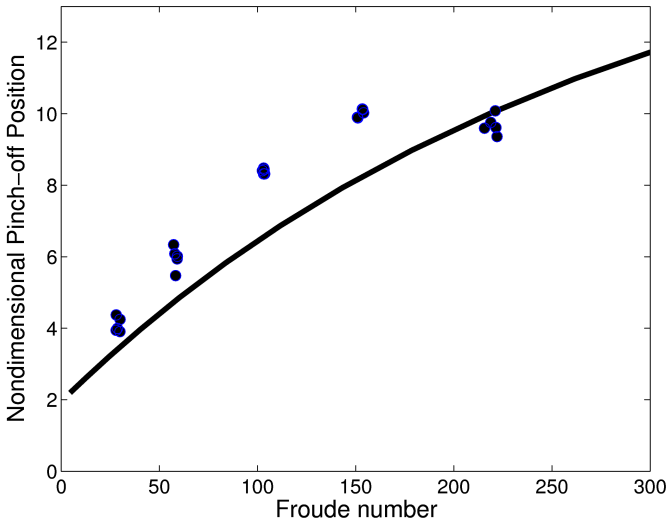

FIGURE 6: The non-dimensional pinch-off depth as a function of the Froude number. The line corresponds to the theoretical model and the dots to the experimental data.

The theoretical cavity profile is a function of the impact velocity and the air-water contact angle. The exact velocities were measured from the high-speed video while the contact angle on the hydrophobic surface was measured in a separate experiment. The 122 degree contact angle results in the parameter α ranging from about 2 to 6 for the velocity ranges investigated. In Fig. 4 the analytical cavity model is plotted over a series of shadowgraph images showing the close agreement between the model and experiments.

To quantitatively compare the theoretical model with experimental data, the time from impact to pinch-off and the depth of the pinch-off event are compared. In Fig. 5 a graph of the non-dimensional pinch-off time as a function of the Froude number for both the cavity model and the experimental data is shown. For low Froude numbers, the model matches the data well, but for larger Froude numbers the model tends to underestimate the pinch-off time. This may be due to the fact that the spheres experience a small deceleration and thus the velocity does not remain constant as the analytical model assumes.

The time to pinch-off remains relatively constant over a large parameter range, so the pinch-off depth acts as a better metric of the accuracy of the model. In Fig. 6 the non-dimensional pinch-off depth of the model and the data are compared. Although the model underestimates the depth for cases with Froude numbers approximately equal to 100 and 150, in general the model accurately estimates the pinch-off depth.

CONCLUSIONS

While free surface impact dynamics have been extensively studied, there are still many aspects of the process that are poorly understood or cannot be analytically described. In this work, several additional terms were added to a theoretical model describing the cavity profile. The terms included forces due to surface tension and pressure and allow the model to be extended past the pinch-off event.

Future work will focus on several areas. First, since the solution of the analytical model strongly depends upon the contact angle of the fluid, experimental and theoretical work will investigate the dynamics of this contact angle and attempt to analytically describe its evolution during the impact process. Additionally the dynamics of the cavity after pinch-off will be studied in order to better characterize the profile and stability of the cavity.

REFERENCES

1. Worthington, A.M. and R.S. Cole, *Impact with a liquid surface studied by the aid of instantaneous photography. Paper II.* Philosophical Transactions of the Royal Society of London. Series A, Containing Papers of a Mathematical or Physical Character, 1900: p. 175–199.
2. Worthington, A.M. and R.S. Cole, *Impact with a Liquid Surface, Studied by the Aid of Instantaneous Photography.* Philosophical Transactions of the Royal Society of London. Series A, Containing Papers of a Mathematical or Physical Character, 1897. **189**: p. 137-148.
3. von Karman, T., *The impact on seaplane floats during landing*. NACA TN, 1929. **321**: p. 2ñ8.
4. Mayo, W.L., *Analysis and modification of theory for impact of seaplanes on water.* NACA Rep, 1945. **810**.
5. Greenhow, M., *Water-Entry and Water-Exit of a Horizontal Circular-Cylinder.* Applied Ocean Research, 1988. **10**(4): p. 191-198.
6. May, A., *Vertical entry of missiles into water.* Journal of Applied Physics, 1952. **23**: p. 1362.
7. May, A., *Water entry and the cavity-running behavior of missiles*. 1975: Storming Media.
8. Glasheen, J.W. and T.A. McMahon, *A hydrodynamic model of locomotion in the basilisk lizard.* Nature, 1996. **380**(6572): p. 340-342.
9. Rosellini, L., et al., *Skipping stones*. Journal of Fluid Mechanics, 2005. **543**: p. 137-146.
10. Clanet, C., F. Hersen, and L. Bocquet, *Secrets of successful stone-skipping*. Nature, 2004. **427**(6969): p. 29-29.
11. Wagner, H., *Phenomena associated with impacts and sliding on liquid surfaces.* Z. Angew. Math. Mech, 1932. **12**: p. 193ñ215.
12. Cointe, R., *Two-dimensional water-solid impact.* Transactions of the ASME. Journal of Offshore Mechanics and Arctic, 1989. **111**(2): p. 109-114.
13. Thexton, A. and J. McGarrick, *Tongue movement of the cat during lapping*. Archives of Oral Biology, 1988. **33**(5): p. 331-339.
14. Eggers, J., *Hydrodynamic theory of forced dewetting.* Physical Review Letters, 2004. **93**(9): p. -.
15. Bonn, D., et al., *Wetting and spreading*. Reviews of Modern Physics, 2009. **81**(2): p. 739-805.
16. Quere, D., *Fluid coating on a fiber.* Annual Review of Fluid Mechanics, 1999. **31**: p. 347-384.
17. Moyo, S. and M. Greenhow, *Free motion of a cylinder moving below and through a free surface.* Applied Ocean Research, 2000. **22**(1): p. 31-44.
18. Liju, P.-Y., R. Machane, and A. Cartellier, *Surge effect during the water exit of an axisymmetric body traveling normal to a plane interface: experiments and BEM*

simulation. Experiments in Fluids, 2001. **31**(3): p. 241-248.
19. Duclaux, V., et al., *Dynamics of transient cavities*. Journal of Fluid Mechanics, 2007. **591**: p. 1-19.
20. Aristoff, J.M. and J.W.M. Bush, *Water entry of small hydrophobic spheres*. Journal of Fluid Mechanics, 2009. **619**: p. 45-78.
21. Grumstrup, T., J.B. Keller, and A. Belmonte, *Cavity ripples observed during the impact of solid objects into liquids*. Physical Review Letters, 2007. **99**(11): p. -.
22. Glasheen, J.W. and T.A. McMahon, *Vertical water entry of disks at low Froude numbers*. Physics of Fluids, 1996. **8**(8): p. 2078-2083.
23. Rayleigh, L., *On the pressure developed in a liquid during the collapse of a spherical cavity*. Phil. Mag, 1917. **34**(200): p. 94–98.
24. Abelson, H.I., *Pressure measurements in the water-entry cavity*. J. Fluid Mech, 1970. **44**(Part 1).
25. Brennen, C., *Cavity surface wave patterns and general appearance*. J. Fluid Mech, 1970. **44**(1): p. 33-49.
26. Brennen, C., *A numerical solution of axisymmetric cavity flows*. J. Fluid Mech, 1969. **37**(4): p. 671-688.